

## Chapter 5: G $\alpha$ s-binding peptides: Directed evolution of G protein class-specific ligands

*Ryan J. Austin<sup>†</sup>, William W. Ja<sup>‡</sup>, and Richard W. Roberts<sup>§\*</sup>*

<sup>†</sup> Department of Biochemistry and Molecular Biophysics, California Institute of Technology, Pasadena, CA 91125

<sup>‡</sup> Division of Biology, California Institute of Technology, Pasadena, CA 91125.

<sup>§</sup> Department of Chemistry and Mork Family Department of Chemical Engineering, University of Southern California, Los Angeles, CA 90089.

\* Corresponding Author: [richrob@usc.edu](mailto:richrob@usc.edu), (213) 821-4132

## ***Abstract***

Heterotrimeric guanine nucleotide-binding proteins (G proteins) are signal transducers, composed of  $\alpha$ ,  $\beta$ , and  $\gamma$  subunits. 19 unique  $G\alpha$  subunits have been identified in humans, which are categorized into 4 classes that describe the downstream effect of a particular signal. Using mRNA display we have isolated  $G\alpha$ s(s)-binding peptides with nanomolar affinities that display subclass binding specificity against a profile of  $G\alpha$  proteins. Our data indicate that selected peptides bind a preferred protein interaction hot spot on  $G\alpha$ , making discriminate contacts with an effector binding region of the subunit. This effector-like mode of peptide recognition presents a mechanistic rationale for the observed activities of selected peptides that is consistent with the lever model of receptor mediated  $G\alpha$  nucleotide exchange. We have presented a strategy for directed evolution of  $G\alpha$  class-specific peptides, demonstrating an 8000-fold inversion in peptide class specificity. Selected ligands offer an attractive tool for the analysis and modulation of G protein signaling networks.

## ***Introduction***

Heterotrimeric guanine-nucleotide binding proteins (G proteins) are signal transducers that route input signals from G protein coupled receptors (GPCRs) to discrete effector pathways with bidirectional specificity. In the basal state, the G protein transducer is heterotrimeric, composed of  $\alpha$ ,  $\beta$ , and  $\gamma$  subunits. Extracellular activation of the GPCR triggers exchange of GDP with GTP in the  $G\alpha$  subunit, causing dissociation of the  $G\beta\gamma$  heterodimer. Both activated  $G\alpha$ -GTP and  $G\beta\gamma$  are capable of regulating effector signaling. The duration of this signal is a function of the GTP phosphohydrolase activity of  $G\alpha$ , which can be accelerated by various GTPase-activating proteins (GAPs). Reassociation of inactivated  $G\alpha$ -GDP with  $G\beta\gamma$  terminates signaling [1].

How a particular signal is routed from GPCR to effector is largely dictated by the identity of the G protein  $\alpha$  subunit. 16 distinct  $G\alpha$  subunit genes have been identified in humans and categorized into four classes (*i/o*, *q/11*, *s*, and *12/13*), which generally describe the effector coupling of the G protein [2]. Cell-specific expression of these  $\alpha$  subunits along with 5  $\beta$  subunits and 12 receptor-specific  $\gamma$  subunits enables differentiated cells to respond uniquely to extracellular signals [3]. The large number of possible combinations of  $\alpha$ ,  $\beta$ , and  $\gamma$  subunits presents investigators with a need for ligands amenable to discriminating these subunits in a class-specific manner. Ligands capable of modulating signaling pathways with a high degree of exclusivity would be useful tools in the study of signaling networks [4] and may offer therapeutic leads for a number of G protein related diseases [5-7].

Design of G $\alpha$  class-specific ligands presents an interesting problem due to the high degree of protein sequence conservation between G $\alpha$  classes and the dynamic topography of the G $\alpha$  binding surface [8]. Combinatorial selection experiments provide a powerful method for solving dynamic binding problems and a number of G protein-binding peptide ligands have been developed using such techniques [9-15]. In a selection experiment a diverse pool of molecules is placed under a selective pressure, such that only fit molecules are retained. In the case of an affinity selection, the selective pressure is target binding. Members of a pool with a high fitness bind tightly to a desired target and these molecules are amplified, coming to dominate the pool after iterative rounds of selective pressure. Techniques for peptide and protein selections such as phage display [16], ribosome display [17], peptides-on-plasmids [18], and the yeast two hybrid system [19], generally involve the physical association of a polypeptide with its encoding nucleic acid, allowing for amplification and identification of selected molecules. mRNA display is an *in vitro* selection technique wherein each peptide in a combinatorial library is covalently coupled to its encoding mRNA as an mRNA-peptide fusion (Fig. 5.1A) [20]. mRNA display allows for routine selection of libraries containing  $>10^{13}$  different polypeptide sequences [21]. This library complexity is significantly greater than that covered by phage display ( $\sim 10^9$ ), and results in selected peptides with binding affinities in the nanomolar to picomolar range [22-26].

We have previously used mRNA display to identify a peptide (R6A), which binds with high affinity to the GDP-bound state of the G $\alpha$ i1 subunit [12]. The R6A peptide exhibits binding affinity for G $\alpha$  subunits within three of the four classes (i/o, q/11, and 12/13), excluding the s-class. A 9 residue core sequence within R6A (R6A-1) is less

selective, demonstrating binding promiscuity across all four classes of G $\alpha$  protein [27]. R6A-1 binds the switch-II/ $\alpha$ -helix 3 (SII/ $\alpha$ 3) site of G $\alpha$ i1 [28], a conserved region that serves as a control site for modulation of G $\alpha$  nucleotide exchange [13]. We reasoned that the R6A-1 sequence could be used as a starting point for the directed evolution of G $\alpha$ -modulating peptides with novel G $\alpha$ -binding specificities. Starting with an mRNA display library incorporating the R6A-1 sequence [15], we have selected peptides with affinity for the short isoform of G $\alpha$ s (G $\alpha$ s(s)), isolating subclass-specific binders that inhibit nucleotide exchange. These peptides retain a consensus EFL-motif, which likely binds across all classes of G $\alpha$  in a conserved manner. The G $\alpha$ s(s) specificity of selected ligands validates our directed evolution strategy and indicates that it will be possible to generate similarly discriminate peptides for a variety of G $\alpha$  subunits.

## Results

### Positive Selection of the G $\alpha$ s(s)-binding Peptide GSP

Our goal in the present work was to develop G $\alpha$ s(s)-specific peptides. To this end, our strategy was to use the promiscuous G $\alpha$ -binding peptide R6A-1 as a starting point for mRNA display selection on G $\alpha$ s(s) target. A scaffolded R6A-1 library (R6A-1-library) was designed to be adaptable to selection on different G $\alpha$  targets, incorporating a 40-50% doped R6A-1 peptide sequence flanked by random amino-acid hexamers (Fig. 5.1B)[15]. To generate G $\alpha$ s(s)-binding peptides, a positive selection of the R6A-1-library was performed on neutravidin beads coated with N-terminally biotinylated G $\alpha$ s(s) (G $\alpha$ s(s)-beads). Here the positive selective pressure was binding to G $\alpha$ s(s); peptide fusions from the R6A-1-library retained on G $\alpha$ s(s)-beads were amplified by PCR and expressed as mRNA-peptide fusions for subsequent rounds of selection. Enrichment of G $\alpha$ s(s)-binding sequences plateaued after 8 rounds of positive selection, as measured by pull-down of [<sup>35</sup>S]Met labeled peptide fusions on G $\alpha$ s(s)-beads (Fig. 5.1B). Discrete peptide sequences from pool 8 were cloned and expressed as biotinylated peptide-maltose-binding protein fusions. Peptide-MBP fusions were immobilized on neutravidin beads (peptide-beads) and screened for binding to soluble [<sup>35</sup>S]Met labeled G $\alpha$ i1 and G $\alpha$ s(s) using a previously developed *in vitro* binding assay. The majority of pool 8 peptide sequences retained affinity for G $\alpha$ i1 equal to or greater than their affinity for G $\alpha$ s(s) in the G $\alpha$ -binding screen. However, one G $\alpha$ s(s)-binding peptide (GSP), representing 5% of the pool 8 sequences screened, bound preferentially to G $\alpha$ s(s).

## **Maturation Selection of $G\alpha s(s)$ -specific mGSP Peptides**

To explore GSP variants with increased  $G\alpha s(s)$ -binding specificity, a GSP-library based on a 50% doped GSP sequence was constructed and subjected to a maturation selection (Fig. 5.1C). This maturation selection was designed to incorporate negative selective pressures against peptides that bind to  $G\alpha i1$ . GSP variants were selected for retention on  $G\alpha s(s)$ -beads in the presence of a molar excess of soluble  $G\alpha i1$  competitor. The concentration of  $G\alpha i1$  competitor and other negative selective pressures were increased over the course of the maturation selection (Experimental Procedures). After 6 rounds of selection, the majority of GSP variants sequenced bound exclusively to  $G\alpha s(s)$  in the  $G\alpha$ -binding screen (Fig. 5.1C). Selected GSP variants were grouped into similar families based on covariant R2L-W6R and L3M-W6R mutations in their core sequences (residues 1-9). Representative peptide variants mGSP-1 (seq: L3M-W6R) and mGSP-2 (seq: R2L-W6R) along with the GSP peptide were synthesized for further analysis.

## **R6A-1 and mGSP Peptides Exhibit an 8000-fold Inversion in $G\alpha i1/G\alpha s(s)$ -Binding Specificity**

We have used surface plasmon resonance (SPR) to measure dissociation constant ( $K_D$ ) values for a matrix of peptide- $G\alpha$  complexes between GSP, mGSP-1, and mGSP-2 peptides and  $G\alpha i1$  and  $G\alpha s(s)$  proteins (Fig. 5.2, Table 5.1). The  $K_D$  matrix charts the course of our two selection step walk: 1) In the positive selection we evolved peptides with increased  $G\alpha s(s)$  affinity, walking through sequence space from the  $G\alpha i1$ -specific R6A-1 peptide to GSP, which exhibits affinity for both  $G\alpha i1$  and  $G\alpha s(s)$  proteins, 2) In the maturation selection we applied a negative  $G\alpha i1$  selective pressure to the GSP-

library, evolving GSP variants that retained affinity for G $\alpha$ s(s), but no longer bound G $\alpha$ i1. G $\alpha$ s(s) peptide binding specificities are quantified in Table 5.1 as the relative free energy stability of the peptide-G $\alpha$ s(s) complex vs. the peptide-G $\alpha$ i1 complex (G $\alpha$ s(s)- $\Delta\Delta G$ ). In sum, the mGSP-1 and mGSP-2 peptides exhibit a 5.4 kcal mol<sup>-1</sup> increase in G $\alpha$ s(s)-binding specificity over R6A-1, equivalent to an 8,000 fold inversion in G $\alpha$ i1/G $\alpha$ s(s) target discrimination.

The 9 residue R6A-1 peptide has been shown to bind the conserved SII/ $\alpha$ 3 effector-binding site of G $\alpha$ i1 [28]. Sequence conservation between R6A-1 and the GSP and mGSP peptides suggests that the presently selected peptides also interact with the SII/ $\alpha$ 3 effector-binding site. Binding site redundancy between R6A-1 and GSP is supported by the finding that R6A-1 directly competes off pull-down of G $\alpha$ i1 on GSP-beads (data not shown). Like R6A-1, the GSP peptide also disrupts formation of the G $\alpha\beta\gamma$  heterotrimer. [<sup>35</sup>S]G $\beta\gamma$  pull-down on both G $\alpha$ i1 and G $\alpha$ s(s) beads is inhibited by the presence of GSP at IC<sub>50</sub> values of 550 nM and 80 nM, respectively (Supplemental Fig. S5.1). Overall, the data support that GSP and mGSP peptides dock near the SII/ $\alpha$ 3 effector-binding site of G $\alpha$ s(s).

### **G $\alpha$ s(s) Subclass-Specific Peptides Exhibit an Effector-like Mode of G $\alpha$ Recognition.**

The binding specificities of GSP and mGSP peptides have been tested against 11 different G $\alpha$  subunits and isoforms (G $\alpha$ : i1, i2, i3, oA, q, 11, 15, s(s), s(l), Olf, and 12) representing the four classes of G $\alpha$  (i/o, q/11, s, 12/13) as well as the small GTPase H-Ras. [<sup>35</sup>S]Met-G $\alpha$  subunits were expressed *in vitro* and assayed for pull-down on peptide-beads to generate a specificity profile for each peptide (Fig. 5.3A). In the pull-down

assays GSP binds  $G\alpha(i/o)$  and  $G\alpha(s)$  classes in a ratio consistent with the SPR data, binding poorly to  $G\alpha(q/11)$  and  $G\alpha(12/13)$ . As expected, the specificity profile of mGSP-1 illustrates a dramatically reduced affinity of the peptide for  $G\alpha(i/o)$  subunits. Surprisingly, GSP and mGSP-1 peptides display subclass-binding specificity to the  $G\alpha(s)$  subunit. Both specificity profiles show reduced binding to the long isoform of  $G\alpha(s)$  ( $G\alpha(s(l))$ ) and minimal binding to the  $G\alpha Olf$  subunit, which shares 77% amino acid sequence identity with  $G\alpha(s)$  (See Supplemental Fig. S5.2 for additional specificity profile data).

We wished to compare the  $G\alpha$  recognition mode of GSP and mGSP-1 peptides with three structurally characterized types of  $G\alpha$ -binding protein: regulator of G protein signaling (RGS) proteins [29, 30]; the GoLoco/G protein regulatory (GPR) motif [31]; and effector proteins [32, 33]. To do this we expressed a series of  $G\alpha i1/G\alpha s(s)$  reciprocal mutants and chimeras, previously developed for the characterization of  $G\alpha$ -binding specificity [34-36], and assayed subunit pull-down on GSP- and mGSP-1-beads (Fig. 5.3B). Pull-down experiments indicate that the recognition mode of GSP and mGSP-1 peptides is distinct from RGS proteins, which make specific contacts at residue Ser206 in  $G\alpha i1$  or the corresponding residue, Asp229 in  $G\alpha s(s)$ . Reciprocal substitution of these residues does not significantly alter peptide binding. Likewise, the manner of peptide recognition is distinct from the GoLoco/GRP regulatory motif, which makes specific contacts with the helical domain of  $G\alpha$ . This is evidenced by the C3 domain chimera ( $G\alpha s(s)(1-185)i1(177-354)$ ), which contains the helical domain of  $G\alpha s(s)$ , but exhibits weaker peptide binding than  $G\alpha i1$ . Rather, peptide recognition appears to be most consistent with effector protein recognition. The C4 chimera ( $G\alpha i1(1-240)s(s)(249-380)$ ),

containing effector-binding elements of  $G\alpha s(s)$ , shows 100% binding to GSP and significant binding to the mGSP-1 peptide. Structural details of an effector-like model of peptide recognition are elaborated upon in the Discussion section.

### **GSP Accelerates Nucleotide Exchange in $G\alpha i1$ and Inhibits Exchange in $G\alpha s(s)$**

We have tested the effect of GSP peptides upon the GDP exchange rate of  $G\alpha i1$  and  $G\alpha s(s)$  using  $[^{35}\text{S}]\text{GTP}\gamma\text{S}$  binding and  $[\gamma^{32}\text{P}]\text{GTP}$  steady-state hydrolysis measurements. In both assays GSP accelerates the rate of nucleotide exchange in  $G\alpha i1$  and inhibits the rate of exchange in  $G\alpha s(s)$ . The association rate of  $[^{35}\text{S}]\text{GTP}\gamma\text{S}$ , which is limited by GDP release, is plotted for  $G\alpha i1$  in the presence of a 10  $\mu\text{M}$  saturating concentration of GSP or a 10  $\mu\text{M}$  suramin control in Figure 5.4A.  $[^{35}\text{S}]\text{GTP}\gamma\text{S}$  binding measurements show GSP acts as a guanine nucleotide exchange factor (GEF) for  $G\alpha i1$ , accelerating the release of GDP four-fold, while suramin inhibits exchange, consistent with its guanine dissociation inhibitor (GDI) activity for both  $G\alpha i1$  and  $G\alpha s(s)$  [37]. The effective GSP concentration required for 50% maximal GEF activity is 290 nM, consistent with the dissociation constant of GSP- $G\alpha i1$  ( $K_D = 280$  nM). GSP has the opposite effect on  $G\alpha s(s)$ . 10  $\mu\text{M}$  GSP inhibits GDP exchange by  $G\alpha s(s)$  three-fold with 50% maximal inhibition at a concentration of 157 nM (Fig. 5.4B), similar to the GSP- $G\alpha s(s)$  dissociation constant ( $K_D = 100$  nM). We also performed steady-state GTP hydrolysis measurements to confirm the peptide activities observed in the  $[^{35}\text{S}]\text{GTP}\gamma\text{S}$  assay. Because GDP release is the rate-limiting step in the guanine nucleotide cycle, perturbations of GDP exchange are evident in the overall steady-state rate, which can be measured as a function of  $[\gamma^{32}\text{P}]\text{GTP}$  hydrolysis. Steady-state hydrolysis measurements

agree with the [<sup>35</sup>S]GTPγS binding experiments, confirming the bifunctional activity of GSP (Fig. 5.4C).

The mGSP-1 and mGSP-2 peptides also inhibit GDP exchange by Gαs(s) in the [<sup>35</sup>S]GTPγS and [<sup>32</sup>P]GTP assays (Supplemental Fig. S5.3). The activity of mGSP-1 and mGSP-2 against Gαi1 proved difficult to determine, however, due to the poor Gαi1 affinity of these peptides. Bifunctional nucleotide exchange activities towards Gαi1 and Gαs(s) proteins have previously been observed for the bee venom peptide melittin [38], as well as, the non-specific peptide KB-752 [39], isolated from *in vitro* selection on Gαi1.

## ***Discussion***

### **Directed Evolution of G $\alpha$ Subclass-Specific Peptides**

The great similarity among G $\alpha$  subunits presents an intriguing problem for the design of G $\alpha$ -specific ligands. Protein sequence identities ranging from 36-52% are observed between the four different classes of G $\alpha$  with subclass identities ranging from 53-93% [40]. This primary sequence identity results in highly conserved G $\alpha$  protein structures with backbone RMS-deviations of  $\sim 1$  Å in the GTPase domains of G $\alpha$ i1, G $\alpha$ q, G $\alpha$ s(s), and G $\alpha$ 12 subunits [32, 41, 42]. We had previously isolated the 9 residue peptide epitope R6A-1 [12], which was shown to bind the highly conserved SII/ $\alpha$ 3 site of G $\alpha$  [28], a region identified as a control site for modulation of G $\alpha$  nucleotide exchange [13]. The R6A-1 peptide exhibited promiscuous binding across all four classes of G $\alpha$ , but the specificity of the peptide could be altered by the addition of flanking residues [27]. Based on these findings, we reasoned that R6A-1 could serve as a starting point for the selection of G $\alpha$ -modulating peptides with novel specificities, thereby using the similarity of G $\alpha$  subunits to our advantage. To select peptides that bound to the SII/ $\alpha$ 3 site of G $\alpha$  with new specificities, we designed an R6A-1-library, incorporating a 40-50% doped R6A-1 core epitope flanked by random peptide hexamers [15]. This scaffolded design predisposed library sequences towards the SII/ $\alpha$ 3 binding site of G $\alpha$ , allowing the sequence space of R6A-1 peptide variants to be interrogated with much greater density than afforded by a purely random, 'naïve' library selection. The R6A-1-library was designed with a 40-50% degeneracy at each residue of the core sequence to mitigate the inherent G $\alpha$ i1-binding specificity of R6A-1, however, it was unclear prior to selection,

what level of specificity could be accommodated within the R6A-1 scaffold. We chose to test our selection strategy by targeting the G $\alpha$ s(s) subunit, which bound R6A-1 with significantly weaker affinity than G $\alpha$ i1.

The R6A-1-library proved amenable to positive selection on G $\alpha$ s(s) target, but the G $\alpha$ i1-binding predisposition of the core epitope precluded selection of high specificity G $\alpha$ s(s)-binders. This is illustrated by the G $\alpha$ i1-binding preference of peptides enriched in the positive selection (Fig. 5.1B) and by a failed selection of the R6A-1-library in the presence of soluble G $\alpha$ i1 competitor (data not shown). A majority of enriched peptide sequences from the positive selection contain 4-5 mutations within the core (Fig 5.1B), representing a relatively long mutational distance. The selected GSP sequence, for instance, contains 5 mutations within the 9 residue core, 3 of which are of low likelihood (D1K [0.7%]; Y4T [1.0%], W5V [1.0%]) based on the theoretical complexity of our pool [43]. The mutagenic probability of generating the GSP core from the R6A-1-library is  $1.9 \times 10^{-10}$ , meaning that in our 10 trillion molecule pool 0, only 1200 full-length copies of the GSP core were present. This copy number is too low to effectively sample the flanking sequences of the R6A-1-library, which explains the recalcitrance of this library to negative G $\alpha$ i1 selective pressure.

To generate peptides with increased G $\alpha$ s(s) specificity, a second selection step was performed using a doped GSP-library. Maturation selection of the GSP-library on G $\alpha$ s(s)-beads in the presence of soluble G $\alpha$ i1 competitor enriched G $\alpha$ s(s)-specific mGSP variants with dramatically reduced G $\alpha$ i1-binding. mGSP sequences show conservation of GSP K1, T4, and V5 residues, and enrichment of the coupled mutations L3M-W6R (mGSP-1) and R2L-W6R (mGSP-2) in the core (Fig. 5.1C). Notably, residues 7-9 of the

core are highly conserved for a consensus EFL-motif, which has been enriched in previous selections against G $\alpha$ i1 [12, 15]. The selected pool of mGSP variants has an average mutational distance from GSP of  $5.6 \pm 1.3$  residues, which is covered by only 1-10 copies of each peptide variant in the GSP-library pool 0 [44]. This long mutational distance suggests that additional selections could generate peptides with even greater G $\alpha$ s(s)-binding specificity.

Using a two-step selection strategy- 1) generating G $\alpha$ i1/G $\alpha$ s(s)-binding promiscuity in the positive selection of GSP, and 2) honing G $\alpha$ s(s) specificity in the maturation selection of mGSP variants- we were able to walk from R6A-1 to the mGSP-1 peptide sequence effecting an 8,000 fold inversion in G $\alpha$ i1/G $\alpha$ s(s)-binding specificity. Directed evolution experiments that evolve binding promiscuity in a first selection step before restricting binding specificity in a second step, are often employed in cases where investigators are unable to comprehensively sample the sequence space of a protein library [45]. The impressive ability of mGSP-1 to discriminate G $\alpha$ s(s) from the 77% identical G $\alpha$ O1f subunit in our pull-down assay suggests that class and even subclass-specific peptides with high affinity can be generated for other G $\alpha$  targets using the directed evolution strategy employed here. Additionally, the selection may be reducible from two steps to one by employing a library scaffold with greater G $\alpha$ -binding flexibility, such as the consensus EFL-motif or a more constrained scaffold like xxhxxWEFL (x = random residue; h = hydrophobic residues V, L, I, or F).

## **Selected Peptides Display Effector-like Recognition of a Proposed G $\alpha$ Hot Spot**

Our data support that GSP and mGSP peptides dock near the SII/ $\alpha$ 3 effector-binding site of G $\alpha$ s(s). It is likely that these peptides bind G $\alpha$  in a manner similar to the non-specific peptide KB-752, previously isolated by phage display selection on G $\alpha$ i1 [13]. KB-752 shares a consensus EFL-motif ('DFL') with selected peptides (Fig. 5.5A) and like GSP, accelerates nucleotide exchange in G $\alpha$ i1 while inhibiting exchange in G $\alpha$ s(s), albeit at higher effective concentrations of 4-5  $\mu$ M [39]. The crystal structure of the KB-752-G $\alpha$ i1 complex has been solved (Fig. 5.5B), showing the peptide binding along the SII/ $\alpha$ 3 cleft of G $\alpha$ i1, burying residues F8 and L9 within an invariant hydrophobic binding pocket composed of conserved residues R208, W211, I212, F215, L249, and I253 in G $\alpha$ i1 [13]. The EFL-motif in GSP and mGSP peptides presumably docks in a similar manner within this hydrophobic pocket, which has been identified as a conserved effector-binding site across all 4 classes of G $\alpha$  [32, 33]. Multiple peptides isolated from *in vitro* selection on G $\alpha$ i1-GDP [12, 13], G $\alpha$ i1-GDP-AIF [14, 15], and now G $\alpha$ s(s)-GDP have been shown to target the SII/ $\alpha$ 3 cleft of G $\alpha$ . The predisposition of this SII/ $\alpha$ 3 site to *in vitro* selection, along with the dynamic nature and high degree of primary sequence conservation within the site (Fig. 5.5C), support that the SII/ $\alpha$ 3 cleft is a protein-protein interaction 'hot spot' [46]. The malleable surfaces of hot spots make these sites difficult to target using structure-based design methods, but amenable to *in vitro* selection approaches [47].

The proposed SII/ $\alpha$ 3 hot spot is a preferred protein interaction surface for a number of natural G $\alpha$ -binding partners. Presently, four models of G $\alpha$ -binding specificity have been developed from crystal structural characterization of G $\alpha$  complexes. These

models are delineated by the classification of  $G\alpha$ -binding partner: 1) RGS proteins [29, 30], 2) the GoLoco/GPR motif [31], 3) effector proteins [32, 33], and 4)  $G\beta\gamma$  heterodimers [48]. A general theme to emerge from the models is that molecular recognition of  $G\alpha$  is bipartite, involving conserved contacts along the SII/ $\alpha$ 3-binding surface that are complemented by specific contacts outside of the SII/ $\alpha$ 3 site. RGS proteins provide a notable exception to this theme, making highly specific contacts at a nonconserved residue ( $G\alpha$ i1-Ser206) within switch-II. To compare the binding specificity of mGSP peptides with structurally characterized models, a series of previously studied  $G\alpha$ i1/ $G\alpha$ s(s) reciprocal mutants [34, 35] and chimeras [36] were expressed and tested for binding to peptide-beads.  $G\alpha$ -binding footprints for RGS4, GoLoco, and the effector protein adenylyl cyclase (AC) are shown in Figure 5.5D. The  $G\beta\gamma$  binding model is not considered in our analysis as  $G\beta\gamma$  generally does not exhibit  $G\alpha$  class-binding specificity.

We considered the 3 remaining models in turn: 1) In the RGS binding model, polar residues from RGS proteins discriminate the primary structure of  $G\alpha$  switches at 5 positions [29, 30]. Reciprocal substitution at one of these positions, Ser206 in  $G\alpha$ i1, with the corresponding residue, Asp229 from  $G\alpha$ s(s), abrogates binding of  $G\alpha$ i/o-specific RGS proteins [30, 34, 35]. Similarly, the Asp229 position of  $G\alpha$ s(s) has been implicated in the  $G\alpha$ s-specific binding of RGS-PX1 [49]. GSP and mGSP-1 binding is not, however, affected by G protein reciprocal substitutions at this position (Fig. 5.3B), indicating that the mechanism of peptide specificity is distinct from RGS binding. 2) In the GoLoco/GPR binding model the GoLoco peptide interacts with both GTPase and helical domains of  $G\alpha$ , docking its N-terminus within the SII/ $\alpha$ 3 cleft [31]. The C-terminus of GoLoco/GPR makes discriminate contacts with the helical domain of  $G\alpha$  in the crystal

structure and functional studies using a series of domain chimeras have demonstrated that these contacts are isoform-specific among G $\alpha$ i subunits [50]. The G $\alpha$ i1/G $\alpha$ s(s) chimera C3, containing a G $\alpha$ s(s) helical domain and G $\alpha$ i1 GTPase domain, shows no pull-down on GSP or mGSP-1, indicating that the peptides are not recognizing the G $\alpha$ s(s) helical domain. 3) In the effector binding model, non-polar effector-residues dock within the hydrophobic pocket formed between the N-termini of SII( $\alpha$ 2) and  $\alpha$ 3 helices (see asterisk in Fig. 5.5B). Specificity determining contacts are made with the C-termini of these helices and the  $\alpha$ 2- $\beta$ 4 and  $\alpha$ 3- $\beta$ 5 effector loops of G $\alpha$  [32, 33]. The C4 chimera, principally composed of G $\alpha$ i1, but containing  $\alpha$ 3 and the  $\alpha$ 3- $\beta$ 5 and  $\alpha$ 4- $\beta$ 6 loops of G $\alpha$ s(s), fully recapitulates G $\alpha$ s(s) pulldown on GSP and recovers mGSP-1 binding. This result suggests that the mGSP-1 peptide discriminates G $\alpha$  targets in an effector-like binding mode via contacts with  $\alpha$ 3 and/or the  $\alpha$ 3- $\beta$ 5 effector loop.

In an effector-like model of peptide recognition, the C-terminus of mGSP-1 (residues 10-15) which is conserved among mGSP variants (Fig. 5.1C), would make discriminate contacts near the  $\alpha$ 3/ $\beta$ 5 loop of G $\alpha$ s(s) in a cooperative fashion with  $\alpha$ 3-binding mGSP-1 core residues. This effector-like mode of mGSP-1 recognition presents a mechanistic rationale for the bifunctional activity of the GSP peptide. *Johnston et al.* [13] have proposed a mechanism for the G $\alpha$ i1 GEF activity of KB-752 wherein peptide binding contacts peel back the switch-II lip of G $\alpha$ i1 (Fig. 5.5B) facilitating nucleotide escape. This proposal is consistent with the G $\beta\gamma$  lever model of GPCR GEF activity [51] and, provided GSP and KB-752 bind the SII-lip in a similar manner, accounts for the G $\alpha$ i1 GEF activity of GSP. However, GSP likely binds G $\alpha$ s(s) at a shifted orientation within the broadened SII/ $\alpha$ 3 cleft, accommodating effector-like specific contacts along

the  $\alpha 3$  helix and  $\alpha 3/\beta 5$  loop. Such a shift would abate contacts between GSP and the SII-lip, occluding nucleotide release, which is consistent with the observed inhibition of GDP exchange in the GSP-G $\alpha$ s(s) complex.

The origins of molecular recognition are difficult to dissect within flexible binding interfaces such as protein-protein interaction hot spots [47] and RNA-protein co-folding sites [52] due to the dynamic cooperativity of the binding fold. Computational methods have proven useful for modeling these interactions [53], but a definitive characterization of binding cooperativity requires combinatorial analysis of residue coupling energies [54-56]. One advantage of *in vitro* selection experiments is that multiple combinatorial solutions are offered for a particular binding problem. Sequence conservation within these solutions can illuminate fundamental binding interaction properties. In the present study, maturation selection has revealed a high degree of sequence conservation within the core and C-terminus of mGSP peptides (residues 1-9,10-15). The finding indicates that these peptide regions are instrumental in G $\alpha$ s(s)-binding, consistent with the proposed effector-like model of peptide recognition. Recent studies of the G $\beta\gamma$  heterodimer integrating *in vitro* selection and structural characterization have linked sub-surfaces on the heterodimer to differential modes of recognition [57]. This type of integrated approach could discern specificity determining contacts within the proposed SII/ $\alpha 3$  hot spot of G $\alpha$ , which may have implications for our understanding of natural binding events, such as the unresolved specific binding of AC isoforms I-C<sub>1</sub>, V-C<sub>1</sub>, and VI-C<sub>1</sub> within the SII/ $\alpha 3$  site of G $\alpha$ i1 [58].

Molecules that specifically inhibit G $\alpha$  proteins are useful tools in the dissection of G protein regulation and may be therapeutic for diseases attributed to G protein activation

[5, 6]. With regard to basic biology, there is presently a discrepancy between G protein subunit specificities measured *in vitro* and those measured in living cells. Fluorescent and luminescent biosensors have proven to be valuable molecules for the real-time tracking and visualization of G protein signal transduction [59-61] and selected natural peptides could be employed in the development of these tools. Our selected peptides also provide leads for the development of treatments to a number of human diseases caused by G $\alpha$ s activation [7, 62]. Constitutive activation of G $\alpha$ s by cholera toxin causes the pathophysiological symptoms of the disease. Separately, hyperactivating mutations of G $\alpha$ s can result in McCune Albright Syndrome (MAS) and are oncogenic in various endocrine cancers [3, 7]. G $\alpha$ s oncogenes have been shown to increase tumorigenicity and metastasis [63] [64], and recent identification of G $\alpha$ s-hyperactivating mutations in kidney cancer indicates that the subunit could be a therapeutic target in developed tumors [65].

## **Experimental Procedures**

### **Materials**

The *Escherichia coli* strains BL21, BL21-(DE3), and BL21-gold were from Novagen (Madison, WI). The G protein expression vector, NpT7-5-H6-TEV-G $\alpha$ i1, was generously provided by Prof. Roger K. Sunahara (University of Michigan). The *in vivo* biotinylation vector, pDW363, was kindly supplied by Dr. David S. Waugh (National Cancer Institute., Frederick MD). Human cDNA clones encoding G proteins were obtained from the UMR cDNA Resource Center ([www.cdna.org](http://www.cdna.org)) in the pcDNA3.1+ vector (Invitrogen). G $\alpha$ i1-rat, G $\alpha$ s(s)-bovine short form chimera constructs were generously provided by Prof. N. Artemyev (University of Iowa). The G $\alpha$  subunits used for the specificity profiles were i1, i2, i3, oA, q, 11, 15, s(s, short isoform), s(l, long isoform), Olf, and 12. G $\alpha$ s(s) residues are referred to in the text with the G $\alpha$ s(l) numbering convention. DNA oligonucleotides were synthesized by *Integrated DNA Technologies, Inc.* (Coralville, IA). Modified and doped oligonucleotides including pF30P were synthesized at *Keck Oligonucleotide Synthesis* (New Haven, CT). DNA sequencing was performed by *Laragen* (Los Angeles, CA). L -[<sup>35</sup>S]-methionine (1175 Ci/mmol), [<sup>35</sup>S]GTP $\gamma$ S (1050 Ci/mmol), and [ $\gamma$ <sup>32</sup>P]GTP (6000 Ci/mmol) were purchased from *MP Biomedicals* (Irvine, CA). Restriction enzymes and T4 DNA ligase were from *New England Biolabs, Inc.* (Beverly, MA).

## G $\alpha$ -subunit Cloning and Expression

Cloning pDW363-H6-G $\alpha$ s(s): pDW363-G $\alpha$ s(s) was modified with an amino-terminal hexahistidine tag by QuikChange (*Stratagene*) PCR using primers pDW363-H6-Top (5' CTT TAA GAA GGA GAT ATA CAT ATG CAC CAC CAT CAC CAT CAC GCT GGA GGC CTG AAC GAT ATT TTC 3') and pDW363-H6-Bottom (5' GAA AAT ATC GTT CAG GCC TCC AGC GTG ATG GTG ATG GTG GTG CAT ATG TAT ATC TCC TTC TTA AAG 3'). A two-stage PCR protocol was adopted to mitigate the effects of primer-dimer formation (150 ng template; 50 °C annealing temperature with a 12 minute extension time at 68 °C; 3 rounds of amplification with primers separated, 19 rounds with pooled reaction)[66]. The pDW363-H6-G $\alpha$ s(s) sequence encodes H6-Nb-G $\alpha$ s(s); the G $\alpha$ s(s) protein with an N-terminal H6 hexahistidine tag followed by a peptide tag that is biotinylated *in vivo*.

Cloning reciprocal mutants: pcDNA3.1+ G $\alpha$ i1 was mutated at residue 206 (Ser206Asp) by QuikChange (*Stratagene*) PCR using primers S206D-Top (5' AAT GTT TGA TGT GGG AGG TCA GAG AGA TGA GCG GAA GAA G 3') and S206D-Bottom (5' CTT CTT CCG CTC ATC TCT CTG ACC TCC CAC ATC AAA CAT T 3'). pcDNA3.1+ G $\alpha$ s(s) was mutated at residue 229 (Asp229Ser) by QuikChange (*Stratagene*) PCR using primers D229S-Top (5' GGG TGG CCA GCG CTC TGA ACG CCG CAA G 3') and D229S-Bottom (5' CTT GCG GCG TTC AGA GCG CTG GCC ACC C 3').

Expression of G $\alpha$ s(s): G $\alpha$ s(s) was recombinantly expressed with some modifications to previously published protocols [67]. A 100 ml Enriched Media culture [2% (w/v) tryptone, 1% (w/v) yeast extract, 0.5% (w/v) NaCl, 0.2% (v/v) glycerol, and

50 mM H<sub>2</sub>PO<sub>4</sub> at pH 7.2, supplemented with 50 µg/ml ampicillin and 50 µM D-biotin] of *E. Coli* BL21(DE3) cells harboring pDW363-H6-Gαs(s) was induced with 0.3 mM IPTG at OD<sub>600</sub> = 0.4, grown at 30 °C for 9 hrs, and pelleted by centrifugation. Pellets were rinsed with ddH<sub>2</sub>O, snap-frozen in dry ice/ethanol, and stored at –80 °C overnight. Cell pellets were resuspended in 15 ml T<sub>50β20P0.1</sub> buffer [50 mM Tris-Cl at pH 8.0, 20 mM β-mercaptoethanol, 0.1 mM phenylmethylsulfonyl fluoride], lysed by Emulsiflex at 5000 psi for 10 min, and centrifuged. Cleared lysate supernatant was applied to a 0.3 ml bed volume Ni-NTA column (*Qiagen*), pre-equilibrated with T<sub>50β20P0.1</sub> /(100 mM NaCl). The column was washed with 3x 2 mL of T<sub>50β20P0.1</sub> /(500 mM NaCl, 10 mM imidazole). Fractions were eluted into T<sub>50β20P0.1</sub> /(50 mM imidazole, 10% glycerol (v/v)), concentrated and exchanged into HGD buffer [50 mM HEPES at pH 7.5, 10% glycerol (v/v), 1 mM DTT] using a Centriprep YM-10 concentrator, and stored at –80 °C. A 100 mL culture yielded 0.1 mg of N-terminally biotinylated Gαs(s) (Nb-Gαs(s)).

Expression of Gαi1: Recombinant rat H6-TEV-Gαi1 (N-terminal hexahistadine tag followed by a TEV protease cut site) was expressed as previously described [12]. Gαi1 was also expressed with an N-terminal peptide tag that is biotinlyated *in vivo* (Nb-Gαi1). A 120 ml LB culture /[50 µg/ml ampicillin, 50 µM D-biotin] of *E. coli* BL21 cells harboring pDW363-Gαi1 was induced with 1 mM IPTG at OD<sub>600</sub> = 0.6, grown at 30 °C for 6 hrs, and pelleted by centrifugation. Cell pellets were rinsed with ddH<sub>2</sub>O, snap-frozen in dry ice/ethanol, and stored at –80 °C overnight. A 30 mL cell pellet was resuspended in 3 mL BPER cell lysis reagent (*Pierce*) at room temperature. The lysate was cleared by centrifugation and incubated with 0.4 ml neutravidin-agarose at 4 °C for 1

hr. The beads were washed 5x with Wash Buffer [1x PBS, 3  $\mu$ M GDP, 2 mM DTT, 0.5% Tween-20 (v/v)] to generate G $\alpha$ i1-beads.

### **mRNA Template Preparation**

Construction of the core-motif R6A-1-library has been described previously [15]. The GSP-library was designed in a similar fashion to incorporate roughly 50% degeneracy per amino-acid residue [43]. The antisense DNA oligo 115.2 (5' AGC AGA CAG ACT AGT GTA ACC GCC 624 621 621 622 612 623 612 211 543 531 613 624 612 632 544 244 632 243 621 514 623 CAT TGT AAT TGT AAA TAG TAA TTG TCC C 3'; numbers denote dNTP mixtures; 1: 70%A, 10%G, 10%C, 10%T; 2: 70%G, 10%A, 10%C, 10%T; 3: 70%C, 10%A, 10%G, 10%T; 4: 70%T, 10%A, 10%G, 10%C; 5: 90%C, 10%G; 6: 50%G, 50%C) was synthesized by Keck Oligonucleotide Synthesis. This oligo was PCR amplified with the forward primer 47T7FP (5' GGA TTC TAA TAC GAC TCA CTA TAG GGA CAA TTA CTA TTT ACA ATT AC 3') and reverse primer 22.9 (5' AGC AGA CAG ACT AGT GTA ACC G 3') to generate the doped GSP-library. The purified dsDNA construct contained a T7 promoter, an untranslated region, and an ORF containing a 3' constant sequence encoding the peptide QLRNSCA. Sequencing of pool 0 demonstrated ~50% degeneracy of the library per doped amino-acid position.

The selection cycle was performed with minor modifications to previously described protocols [12]. Transcription reactions [80 mM HEPES-KOH at pH 7.5, 2 mM spermidine, 40 mM DTT, 25 mM MgCl<sub>2</sub>, 4 mM each of ATP, CTP, GTP, and UTP, and 10  $\mu$ g/mL DNA template] were treated with RNasecure (*Ambion, Inc.*, Austin, TX) prior to initiating the reaction with T7 RNA polymerase [68]. After a 4 h incubation at 37 °C,

transcription reactions were spiked with 30  $\mu$ l of DNaseI (*Epicenter*) and incubated an additional 30 minutes. Reactions were quenched with 0.1 volume of 0.5 M EDTA, phenol-extracted using Phase Lock Gel (*Brinkmann Instruments, Inc.*, Westbury, NY), and desalted by 2-propanol precipitation. A fraction of the purified RNA was treated with DNaseI (*Invitrogen*) following the manufacturer's specifications, quenched with EDTA, phenol-extracted and precipitated similarly.

The puromycin-DNA linker, pF30P (5'dA<sub>21</sub>[S9]<sub>2</sub>dAdCdC-P; S = spacer phosphoramidite 9; P = CPG-puromycin; 5'- phosphorylated using phosphorylation reagent II; *Glen Research Corp.*, Sterling, VA) was ligated to mRNA templates using a splint oligo (5' TTT TTT TTT TTN AGC AGA CAG AC 3'). RNA [10  $\mu$ M], splint, and pF30P (1:1.1:0.5, respectively) were hybridized by heating at 95 °C for 3 min, adding T4 DNA ligase buffer (1x final concentration), and cooling on ice for 10 min. SUPERase-In [1 unit/ $\mu$ L](*Ambion*) and T4 DNA ligase (1.6 units/pmol mRNA) were added and the reaction was incubated at room temperature for 2 h. Ligated mRNA-F30P was purified by denaturing UREA-PAGE, collected from excised gel pieces by passive diffusion in water, and desalted by ethanol precipitation.

### **mRNA Display Selection**

Purified mRNA-F30P templates were translated in rabbit reticulocyte lysate (Red Nova lysate, *Novagen*) with L-[<sup>35</sup>S]-methionine labeling under optimized conditions [100 mM KOAc, 0.5 mM MgOAc, 1 unit/ $\mu$ l SUPERase-In, and 0.5  $\mu$ M mRNA-F30P] and supplemented with unlabeled L-methionine [0.5 mM]. Reactions were incubated for 1 h at 30 °C, quenched by addition of KOAc [585 mM] and MgCl<sub>2</sub> [50 mM], and incubated

on ice 15 min to facilitate RNA-peptide fusion formation [69]. RNA-peptide fusions were purified by dilution into a 100-fold excess of 1x isolation buffer [50 mM HEPES-KOH at pH 7.5, 1 M NaCl, 1 mM EDTA, 1 mM  $\beta$ -mercaptoethanol, and 0.05% (v/v) Tween-20 (*Biorad*)] containing prewashed dT-cellulose (*New England Biolabs*). Mixtures were rotated at 4 °C for 1 h and oligo dT-cellulose was washed with 0.4x isolation buffer in a cellulose acetate 0.45- $\mu$ m centrifuge tube filter (Costar Spin-X, *Corning, Inc.*, Corning, NY). RNA-peptide fusions were eluted with warm ddH<sub>2</sub>O / [1 mM  $\beta$ -mercaptoethanol]. Fusions were 2-propanol-precipitated with linear acrylamide (*Ambion*) as a carrier and subsequently reverse transcribed (Superscript II, *Invitrogen Corp.*, Carlsbad, CA) with the reverse primer 22.9 to generate RT-fusions.

The Gas(s)-beads were prepared immediately prior to use in selections. Nb-Gas(s) (15-30  $\mu$ g) was rotated with 30  $\mu$ l bed volume of neutravidin-agarose (*Pierce*) in 0.5 mL wash buffer [1x PBS, 3  $\mu$ M GDP, 2 mM DTT, 0.5% Tween-20 (v/v)] at 4 °C for 1 h. Beads were washed with wash buffer and resuspended in Binding Buffer [25 mM HEPES-KOH at pH 7.5, 150 mM NaCl, 1 mM  $\beta$ -mercaptoethanol, 10  $\mu$ M GDP, 1 mM EDTA, 5 mM MgCl<sub>2</sub>, 0.05% (v/v) Tween-20] supplemented with 1 mM D-biotin [0.1 mM] and rotated for an additional 10 minutes to block biotin-binding sites. Beads were then washed thoroughly with Selection Buffer [25 mM HEPES-KOH at pH 7.5, 150 mM NaCl, 1 mM  $\beta$ -mercaptoethanol, 10  $\mu$ M GDP, 1 mM EDTA, 5 mM MgCl<sub>2</sub>, 0.05% (v/v) Tween-20, 0.05% (w/v) BSA (electrophoresis-grade, *Sigma*), 1  $\mu$ g/mL yeast tRNA (*Roche Diagnostics Corp.*, Indianapolis, IN)] and rotated with RT-fusions in 1 mL Selection Buffer, at 4 °C for 1 h. The matrix was then washed with 4x 0.5 mL of Selection Buffer followed by 2x 0.5 mL of Binding Buffer. Bound fusions were eluted

with 2x 0.1 mL of 0.15% (w/v) SDS using a 0.45- $\mu$ m centrifuge tube filter. SDS was removed using SDS-OUT (*Pierce*) following manufacturers specifications, and cDNA was ethanol-precipitated with linear acrylamide (*Ambion*). PCR amplification of the cDNA with primers 47T7FP and 22.9 generated the dsDNA template for the next round of selection. DNA templates could also be cloned into pDW363C for sequencing.

Additional negative G $\alpha$ 1 selective pressures were applied during the maturation selection. RT-fusions were sieved through a column of G $\alpha$ 1-beads (0.3 mL bed volume equilibrated in Selection Buffer) prior to incubation with G $\alpha$ s(s)-beads. Incubation of the pre-sieved RT-fusion and G $\alpha$ s(s)-beads was performed in Selection Buffer supplemented with soluble G $\alpha$ 1 competitor at a concentration ranging from 10  $\mu$ g/mL in round 1 (R1) of selection, to 20  $\mu$ g/mL (R2), to 40  $\mu$ g/mL (R3-R6). Washes of the G $\alpha$ s(s)-beads after incubation with pre-sieved RT-fusions were conducted in Selection Buffer supplemented with 20  $\mu$ g/mL soluble G $\alpha$ 1 competitor (R3-R6). Binding assays between [<sup>35</sup>S]Met-peptide fusions and G $\alpha$ 1-beads or G $\alpha$ s(s)-beads were performed as previously described [12].

### **Cloning and Expression of Selected Peptides**

Selected pools were cloned into the biotinylation vector pDW363C [27] for sequencing and expression. Pool dsDNA was PCR-amplified using universal primer 29.4 (5' TGA AGT CTG GAG TAT TTA CAA TTA CAA TG 3') and reverse primer 22.9 (5' AGC AGA CAG ACT AGT GTA ACC G 3'), digested with *BpmI/SpeI*, and ligated to pDW363C (digested with *BseRI/SpeI*). Ligations were digested with *KpnI* to reduce

vector-only contaminant, transformed into the BL21 gold (*Stratagene*) *E. coli* cell line, and plated on LB-Amp. Individual colonies were picked for sequencing.

Selected peptides were expressed as maltose-binding protein (MBP) fusions using the *in vivo* biotinylation system pDW363C (Nb-(Factor Xa site)-peptide-MBP). Expression and cell lysate preparation of pDW363C clones, as well as MBP and R6A-MBP controls, were performed as described above. Nb-peptide-MBP was purified directly onto neutravidin-agarose to generate peptide-beads for the G $\alpha$  binding screen and G $\alpha$  specificity profiles. For applications requiring removal of the biotin tag (Nb) from the peptide, Factor Xa was used following previously published protocols [12]. Briefly, cleared lysate was purified on streptavidin sepharose (High Performance, *Amersham*) and washed 5x with pDW buffer [50 mM HEPES-KOH at pH 7.5, 200 mM NaCl, 1 mM EDTA, and 0.1% Triton X-100] followed by a 2x wash with Xa buffer [50 mM HEPES-KOH at pH 7.5, 150 mM NaCl, and 1 mM CaCl<sub>2</sub>]. Protein was incubated overnight with Factor Xa (20 units, *Amersham*) in Xa buffer at room temperature and eluted with pDW buffer. Factor Xa was removed with p-aminobenzamidine agarose (*Sigma*). Purified proteins were desalted and concentrated in a Centriprep YM-30 into 1x PBS.

### **G $\alpha$ Binding Screen and Specificity Profile Assay**

[<sup>35</sup>S]Met-labeled G protein subunits were translated discreetly in coupled transcription/translation reactions using the TNT reticulocyte lysate system (T7 promoter, *Promega*, Madison, WI). Typically 0.3-1.0  $\mu$ g of plasmid DNA and 25  $\mu$ Ci of L-[<sup>35</sup>S]-methionine were used per 25  $\mu$ l reaction. Reactions were desalted and exchanged using

MicroSpin G-25 columns (*GE Healthcare*) into buffer [50 mM HEPES-KOH at pH 7.5, 6 mM MgCl<sub>2</sub>, 75 mM sucrose, 1 mM EDTA, 1 μM GDP, and 0.5% (v/v) Tween-20] and reaction yields were quantitated by trichloroacetic acid precipitation of a 2-μl aliquot of each reaction.

The Gα interaction assay was performed as described previously [27]. Individual binding reactions were assembled with equivalent aliquots of desalted Gα subunits in 0.5 mL Binding buffer / (0.5% (w/v) BSA) containing 10 μl of peptide-beads. After rotating at 4 °C for 1 h, beads were washed 3x with 0.5 mL binding buffer using a 0.45-μm spin filter tube, and transferred to a vial for scintillation counting. Assays with aluminum fluoride were performed similarly, except that binding buffer was supplemented with 10 mM NaF and 25 μM AlCl<sub>3</sub>.

### **Binding Analysis by Surface Plasmon Resonance**

Kinetic measurements were conducted at 25 °C on a Biacore 2000 instrument (*Biacore, Inc.*, Piscataway, NJ) as described previously [12]. Nb-Gas(s) and Nb-Gai1 were immobilized on research-grade SA (streptavidin) sensor chips at a surface density of ~ 1000 response units. A concentration series (0, 10, 30, 90, 270, 810, and 2430 nM) of each peptide analyte in modified HBS-EP running buffer [10 mM HEPES at pH 7.4, 150 mM NaCl, 3 mM EDTA, 0.005% (v/v) Tween-20, 2 mM MgCl<sub>2</sub>, 30 μM GDP, 0.05% (w/v) BSA and 0-0.5% DMSO] was injected across the chip for 2 min at 100 μl/min, followed by a 6 min dissociation period. K<sub>D</sub> values for peptides were calculated from rates determined by CLAMP.

## **G $\alpha$ nucleotide Cycle Assays**

GTP $\gamma$ S exchange assays were performed using a nitrocellulose filter binding method [70] at either 20 °C (G $\alpha$ s(s)) or 30 °C (G $\alpha$ i1). Briefly, G $\alpha$  was diluted into HEDT buffer [50 mM HEPES-NaOH at pH 7.6, 1 mM EDTA, 1 mM DTT, 0.01% Tween-20] to a final concentration of 250 nM (1 pmol/10  $\mu$ l assay) on ice. The reaction was started by adding 4 volumes (40  $\mu$ l/assay) of reaction buffer [50 mM HEPES-NaOH at pH 7.6, 1 mM EDTA, 1 mM DTT, 12.5 mM MgSO<sub>4</sub>, 0.2-1.2  $\mu$ M [<sup>35</sup>S]GTP $\gamma$ S (50-200 cpm/fmol), 0.01% Tween-20] with or without test peptide. The reactions were stopped by withdrawing duplicate aliquots (50  $\mu$ l/assay), diluting these into 10 mL ice-cold Stop Buffer [Tris-HCl at pH 8.0, 100 mM NaCl, 25 mM MgCl<sub>2</sub>, 100  $\mu$ M GTP], and immediately filtering over HA-85 nitrocellulose membranes (*Whatman*). Equilibrium experiments were conducted similarly, with the exception that G $\alpha$  subunits were pre-incubated for 10 min with or without peptide on ice prior to initiating reactions. Data from kinetic experiments were processed by non-linear, least squares curve fitting to a pseudo first-order association rate. Concentration response curves were fit to a 3 parameter logistic equation. All measurements were performed multiple times.

Steady-State [ $\gamma$ <sup>32</sup>P]GTP assays were undertaken using a charcoal precipitation based method [71] at either 20 °C (G $\alpha$ s(s)) or 30 °C (G $\alpha$ i1). G $\alpha$  proteins were diluted on ice to 200 nM (2x desired concentration) in assay buffer [20 mM NaHEPES pH 8.0; 100mM NaCl; 1 mM EDTA; 2 mM MgCl<sub>2</sub>; 1 mM DTT; 0.05% Tween-20]. GTPase reactions were initiated by addition of an equal volume of assay buffer containing a 2x concentration of [ $\gamma$ <sup>32</sup>P]GTP 0.3-1  $\mu$ M (1000-3000 cpm/fmol);  $\pm$  peptide. Duplicate

aliquots (50  $\mu$ l) were removed at timed intervals and quenched with 900  $\mu$ L of ice-cold 5% (w/v) activated charcoal in 50 mM  $\text{NaH}_2\text{PO}_4$ . Quenched reactions were centrifuged for 10 min at 8000 x g and duplicate 100  $\mu$ l aliquots of the resultant supernatant were subjected to scintillation counting to quantify released [ $^{32}\text{P}$ i].

## ***Acknowledgements***

We would like to thank N. O. Artemyev for providing the G $\alpha$ 1/G $\alpha$ s(s) chimeras; R. T. Sunahara for the TEV protein expression vector; D. S. Waugh for the original pDW363 vector; and P. J. Bjorkman for the use of the Biacore 2000 instrument. Thanks to T. T. Takahashi for helpful discussion. This work was supported by funding from the National Institutes of Health (GM60416) and the Beckman Foundation.

## References

1. Birnbaumer, L. Ed. (2004). Signal transduction by G proteins: basic principles, molecular diversity, and structural basis of their actions. (Boston, MA: Academic).
2. Neves, S.R., Ram, P.T., and Iyengar, R. (2002). G protein pathways. *Science* 296, 1636-1639.
3. Wettschureck, N., and Offermanns, S. (2005). Mammalian G proteins and their cell type specific functions. *Physiol Rev* 85, 1159-1204.
4. Jordan, J.D., Landau, E.M., and Iyengar, R. (2000). Signaling networks: the origins of cellular multitasking. *Cell* 103, 193-200.
5. Holler, C., Freissmuth, M., and Nanoff, C. (1999). G proteins as drug targets. *Cell Mol Life Sci* 55, 257-270.
6. Freissmuth, M., Waldhoer, M., Bofill-Cardona, E., and Nanoff, C. (1999). G protein antagonists. *Trends Pharmacol Sci* 20, 237-245.
7. Spiegel, A.M., and Weinstein, L.S. (2004). Inherited diseases involving G proteins and G protein-coupled receptors. *Annu Rev Med* 55, 27-39.
8. Ja, W.W., and Roberts, R.W. (2005). G-protein-directed ligand discovery with peptide combinatorial libraries. *Trends Biochem Sci* 30, 318-324.
9. Martin, E.L., Rens-Domiano, S., Schatz, P.J., and Hamm, H.E. (1996). Potent peptide analogues of a G protein receptor-binding region obtained with a combinatorial library. *J Biol Chem* 271, 361-366.
10. Scott, J.K., Huang, S.F., Gangadhar, B.P., Samoriski, G.M., Clapp, P., Gross, R.A., Taussig, R., and Smrcka, A.V. (2001). Evidence that a protein-protein interaction 'hot spot' on heterotrimeric G protein betagamma subunits is used for recognition of a subclass of effectors. *Embo J* 20, 767-776.
11. Hessling, J., Lohse, M.J., and Klotz, K.N. (2003). Peptide G protein agonists from a phage display library. *Biochem Pharmacol* 65, 961-967.
12. Ja, W.W., and Roberts, R.W. (2004). In vitro selection of state-specific peptide modulators of G protein signaling using mRNA display. *Biochemistry* 43, 9265-9275.
13. Johnston, C.A., Willard, F.S., Jezyk, M.R., Fredericks, Z., Bodor, E.T., Jones, M.B., Blaesius, R., Watts, V.J., Harden, T.K., Sondek, J., Ramer, J.K., and Siderovski, D.P. (2005). Structure of Galpha(i1) bound to a GDP-selective peptide provides insight into guanine nucleotide exchange. *Structure* 13, 1069-1080.
14. Johnston, C.A., Lobanova, E.S., Shavkunov, A.S., Low, J., Ramer, J.K., Blaesius, R., Fredericks, Z., Willard, F.S., Kuhlman, B., Arshavsky, V.Y., and Siderovski, D.P. (2006). Minimal Determinants for Binding Activated Galpha from the Structure of a Galpha(i1)-Peptide Dimer. *Biochemistry* 45, 11390-11400.
15. Ja, W.W., Wiser, O., Austin, R.J., Jan, L.Y., and Roberts, R.W. (2006). Turning G Proteins On and Off Using Peptide Ligands. *ACS Chemical Biology* 1, 570-574.
16. Smith, G.P., and Petrenko, V.A. (1997). Phage Display. *Chem Rev* 97, 391-410.

17. Hanes, J., and Pluckthun, A. (1997). In vitro selection and evolution of functional proteins by using ribosome display. *Proc Natl Acad Sci U S A* *94*, 4937-4942.
18. Cull, M.G., Miller, J.F., and Schatz, P.J. (1992). Screening for receptor ligands using large libraries of peptides linked to the C terminus of the lac repressor. *Proc Natl Acad Sci U S A* *89*, 1865-1869.
19. Fields, S., and Song, O. (1989). A novel genetic system to detect protein-protein interactions. *Nature* *340*, 245-246.
20. Roberts, R.W., and Szostak, J.W. (1997). RNA-peptide fusions for the in vitro selection of peptides and proteins. *Proc Natl Acad Sci U S A* *94*, 12297-12302.
21. Takahashi, T.T., Austin, R.J., and Roberts, R.W. (2003). mRNA display: ligand discovery, interaction analysis and beyond. *Trends Biochem Sci* *28*, 159-165.
22. Wilson, D.S., Keefe, A.D., and Szostak, J.W. (2001). The use of mRNA display to select high-affinity protein-binding peptides. *Proc Natl Acad Sci U S A* *98*, 3750-3755.
23. Keefe, A.D., and Szostak, J.W. (2001). Functional proteins from a random-sequence library. *Nature* *410*, 715-718.
24. Austin, R.J., Xia, T., Ren, J., Takahashi, T.T., and Roberts, R.W. (2002). Designed Arginine-Rich RNA-Binding Peptides with Picomolar Affinity. *J. Am. Chem. Soc.* *124*, 10966-10967.
25. Raffler, N.A., Schneider-Mergener, J., and Famulok, M. (2003). A novel class of small functional peptides that bind and inhibit human alpha-thrombin isolated by mRNA display. *Chem Biol* *10*, 69-79.
26. Getmanova, E.V., Chen, Y., Bloom, L., Gokemeijer, J., Shamah, S., Warikoo, V., Wang, J., Ling, V., and Sun, L. (2006). Antagonists to human and mouse vascular endothelial growth factor receptor 2 generated by directed protein evolution in vitro. *Chem Biol* *13*, 549-556.
27. Ja, W.W., Adhikari, A., Austin, R.J., Sprang, S.R., and Roberts, R.W. (2005). A peptide core motif for binding to heterotrimeric G protein alpha subunits. *J Biol Chem* *280*, 32057-32060.
28. Willard, F.S., and Siderovski, D.P. (2006). The R6A-1 peptide binds to switch II of Galpha1 but is not a GDP-dissociation inhibitor. *Biochem Biophys Res Commun* *339*, 1107-1112.
29. Tesmer, J.J., Berman, D.M., Gilman, A.G., and Sprang, S.R. (1997). Structure of RGS4 bound to AlF4-activated G(i alpha1): stabilization of the transition state for GTP hydrolysis. *Cell* *89*, 251-261.
30. Slep, K.C., Kercher, M.A., He, W., Cowan, C.W., Wensel, T.G., and Sigler, P.B. (2001). Structural determinants for regulation of phosphodiesterase by a G protein at 2.0 Å. *Nature* *409*, 1071-1077.
31. Kimple, R.J., Kimple, M.E., Betts, L., Sondek, J., and Siderovski, D.P. (2002). Structural determinants for GoLoco-induced inhibition of nucleotide release by Galpha subunits. *Nature* *416*, 878-881.
32. Tesmer, V.M., Kawano, T., Shankaranarayanan, A., Kozasa, T., and Tesmer, J.J. (2005). Snapshot of activated G proteins at the membrane: the Galphaq-GRK2-Gbetagamma complex. *Science* *310*, 1686-1690.

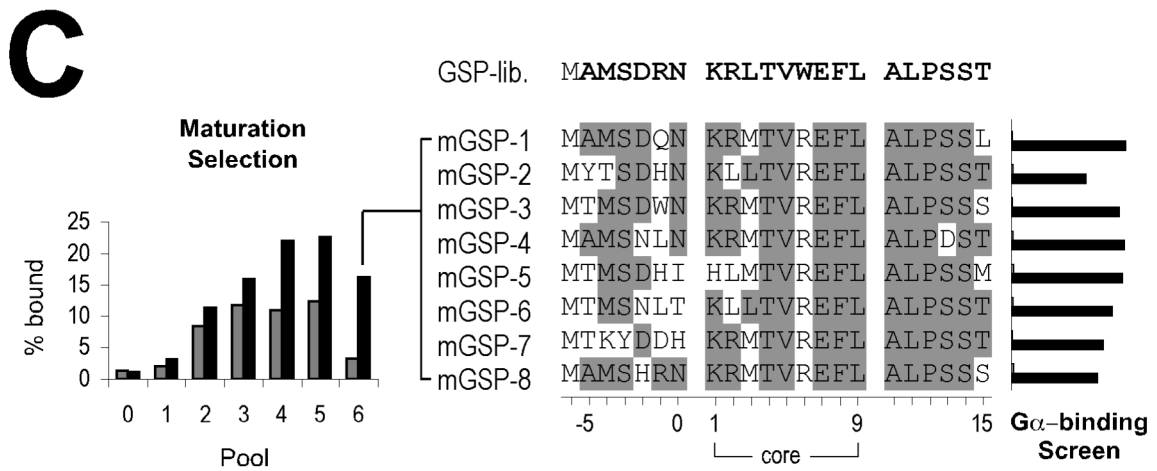
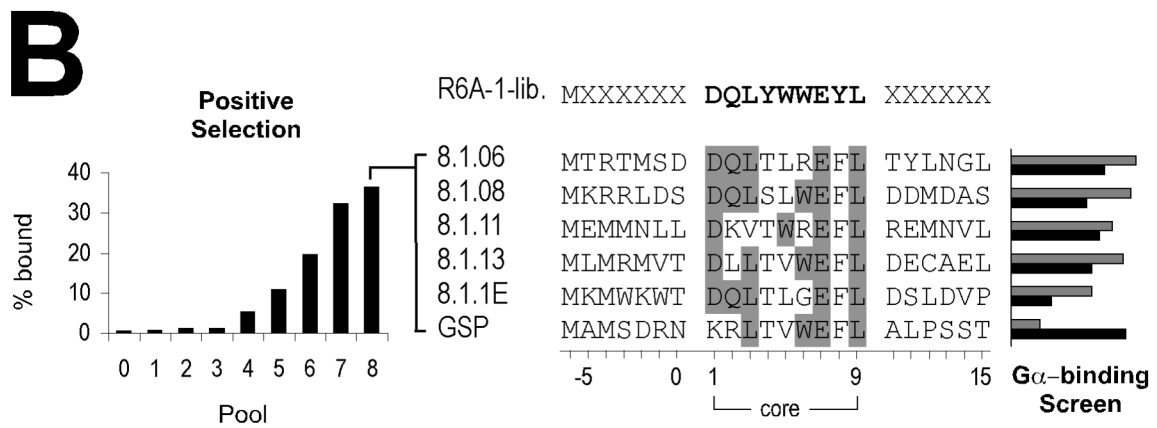
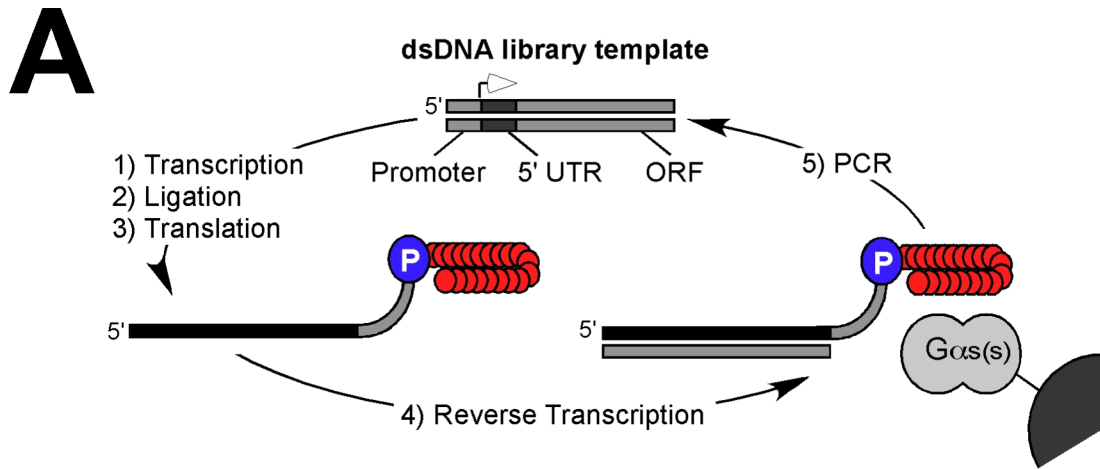
33. Chen, Z., Singer, W.D., Sternweis, P.C., and Sprang, S.R. (2005). Structure of the p115RhoGEF rgRGS domain-Galphi13/i1 chimera complex suggests convergent evolution of a GTPase activator. *Nat Struct Mol Biol* 12, 191-197.
34. Natochin, M., and Artemyev, N.O. (1998). Substitution of transducin ser202 by asp abolishes G-protein/RGS interaction. *J Biol Chem* 273, 4300-4303.
35. Woulfe, D.S., and Stadel, J.M. (1999). Structural basis for the selectivity of the RGS protein, GAIP, for Galphi family members. Identification of a single amino acid determinant for selective interaction of Galphi subunits with GAIP. *J Biol Chem* 274, 17718-17724.
36. Natochin, M., Gasimov, K.G., and Artemyev, N.O. (2002). A GPR-protein interaction surface of Gi(alpha): implications for the mechanism of GDP-release inhibition. *Biochemistry* 41, 258-265.
37. Freissmuth, M., Boehm, S., Beindl, W., Nickel, P., Ijzerman, A.P., Hohenegger, M., and Nanoff, C. (1996). Suramin analogues as subtype-selective G protein inhibitors. *Mol Pharmacol* 49, 602-611.
38. Fukushima, N., Kohno, M., Kato, T., Kawamoto, S., Okuda, K., Misu, Y., and Ueda, H. (1998). Melittin, a metabostatic peptide inhibiting Gs activity. *Peptides* 19, 811-819.
39. Johnston, C.A., Ramer, J.K., Blaesius, R., Fredericks, Z., Watts, V.J., and Siderovski, D.P. (2005). A bifunctional Galphi/Galphas modulatory peptide that attenuates adenylyl cyclase activity. *FEBS Lett* 579, 5746-5750.
40. Downes, G.B., and Gautam, N. (1999). The G protein subunit gene families. *Genomics* 62, 544-552.
41. Sunahara, R.K., Tesmer, J.J., Gilman, A.G., and Sprang, S.R. (1997). Crystal structure of the adenylyl cyclase activator Galpha. *Science* 278, 1943-1947.
42. Kreutz, B., Yau, D.M., Nance, M.R., Tanabe, S., Tesmer, J.J., and Kozasa, T. (2006). A new approach to producing functional G alpha subunits yields the activated and deactivated structures of G alpha(12/13) proteins. *Biochemistry* 45, 167-174.
43. LaBean, T.H., and Kauffman, S.A. (1993). Design of synthetic gene libraries encoding random sequence proteins with desired ensemble characteristics. *Protein Sci* 2, 1249-1254.
44. Knight, R., and Yarus, M. (2003). Analyzing partially randomized nucleic acid pools: straight dope on doping. *Nucleic Acids Res* 31, e30.
45. Dalby, P.A. (2003). Optimising enzyme function by directed evolution. *Curr Opin Struct Biol* 13, 500-505.
46. Clackson, T., and Wells, J.A. (1995). A hot spot of binding energy in a hormone-receptor interface. *Science* 267, 383-386.
47. Ma, B., Wolfson, H.J., and Nussinov, R. (2001). Protein functional epitopes: hot spots, dynamics and combinatorial libraries. *Curr Opin Struct Biol* 11, 364-369.
48. Wall, M.A., Posner, B.A., and Sprang, S.R. (1998). Structural basis of activity and subunit recognition in G protein heterotrimers. *Structure* 6, 1169-1183.
49. Zheng, B., Ma, Y.C., Ostrom, R.S., Lavoie, C., Gill, G.N., Insel, P.A., Huang, X.Y., and Farquhar, M.G. (2001). RGS-PX1, a GAP for Galphas and sorting nexin in vesicular trafficking. *Science* 294, 1939-1942.

50. Mittal, V., and Linder, M.E. (2004). The RGS14 GoLoco domain discriminates among Galphai isoforms. *J Biol Chem* 279, 46772-46778.
51. Rondard, P., Iiri, T., Srinivasan, S., Meng, E., Fujita, T., and Bourne, H.R. (2001). Mutant G protein alpha subunit activated by Gbeta gamma: a model for receptor activation? *Proc Natl Acad Sci U S A* 98, 6150-6155.
52. Das, C., and Frankel, A.D. (2003). Sequence and structure space of RNA-binding peptides. *Biopolymers* 70, 80-85.
53. DeLano, W.L. (2002). Unraveling hot spots in binding interfaces: progress and challenges. *Curr Opin Struct Biol* 12, 14-20.
54. Schreiber, G., and Fersht, A.R. (1995). Energetics of protein-protein interactions: analysis of the barnase-barstar interface by single mutations and double mutant cycles. *J Mol Biol* 248, 478-486.
55. Kranz, J.K., and Hall, K.B. (1999). RNA recognition by the human U1A protein is mediated by a network of local cooperative interactions that create the optimal binding surface. *J Mol Biol* 285, 215-231.
56. Austin, R.J., Xia, T., Ren, J., Takahashi, T.T., and Roberts, R.W. (2003). Differential modes of recognition in N peptide-boxB complexes. *Biochemistry* 42, 14957-14967.
57. Davis, T.L., Bonacci, T.M., Sprang, S.R., and Smrcka, A.V. (2005). Structural and molecular characterization of a preferred protein interaction surface on G protein beta gamma subunits. *Biochemistry* 44, 10593-10604.
58. Dessauer, C.W., Tesmer, J.J., Sprang, S.R., and Gilman, A.G. (1998). Identification of a Galpha binding site on type V adenylyl cyclase. *J Biol Chem* 273, 25831-25839.
59. Janetopoulos, C., Jin, T., and Devreotes, P. (2001). Receptor-mediated activation of heterotrimeric G-proteins in living cells. *Science* 291, 2408-2411.
60. Hamdan, F.F., Audet, M., Garneau, P., Pelletier, J., and Bouvier, M. (2005). High-throughput screening of G protein-coupled receptor antagonists using a bioluminescence resonance energy transfer 1-based beta-arrestin2 recruitment assay. *J Biomol Screen* 10, 463-475.
61. Gibson, S.K., and Gilman, A.G. (2006). Galpha and Gbeta subunits both define selectivity of G protein activation by alpha2-adrenergic receptors. *Proc Natl Acad Sci U S A* 103, 212-217.
62. Weinstein, L.S., Liu, J., Sakamoto, A., Xie, T., and Chen, M. (2004). Minireview: GNAS: normal and abnormal functions. *Endocrinology* 145, 5459-5464.
63. Chien, J., Wong, E., Nikes, E., Noble, M.J., Pantazis, C.G., and Shah, G.V. (1999). Constitutive activation of stimulatory guanine nucleotide binding protein (G(S)alphaQL)-mediated signaling increases invasiveness and tumorigenicity of PC-3M prostate cancer cells. *Oncogene* 18, 3376-3382.
64. Regnauld, K., Nguyen, Q.D., Vakaet, L., Bruyneel, E., Launay, J.M., Endo, T., Mareel, M., Gespach, C., and Emami, S. (2002). G-protein alpha(olf) subunit promotes cellular invasion, survival, and neuroendocrine differentiation in digestive and urogenital epithelial cells. *Oncogene* 21, 4020-4031.
65. Kalfa, N., Lumbroso, S., Boulle, N., Guiter, J., Soustelle, L., Costa, P., Chapuis, H., Baldet, P., and Sultan, C. (2006). Activating mutations of Gsalphai in kidney cancer. *J Urol* 176, 891-895.

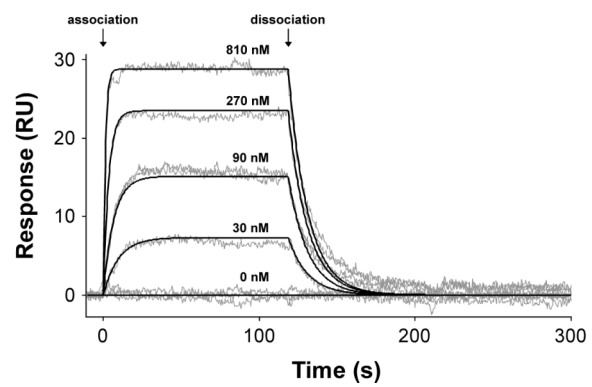
66. Wang, W., and Malcolm, B.A. (1999). Two-stage PCR protocol allowing introduction of multiple mutations, deletions and insertions using QuikChange Site-Directed Mutagenesis. *Biotechniques* 26, 680-682.
67. Lee, E., Linder, M.E., and Gilman, A.G. (1994). Expression of G-protein alpha subunits in *Escherichia coli*. *Methods Enzymol* 237, 146-164.
68. Milligan, J.F., and Uhlenbeck, O.C. (1989). Synthesis of small RNAs using T7 RNA polymerase. *Methods Enzymol* 180, 51-62.
69. Liu, R., Barrick, J.E., Szostak, J.W., and Roberts, R.W. (2000). Optimized synthesis of RNA-protein fusions for in vitro protein selection. *Methods Enzymol* 318, 268-293.
70. Nanoff, C., Kudlacek, O., and Freissmuth, M. (2002). Development of Gs-selective inhibitory compounds. *Methods Enzymol* 344, 469-480.
71. Ross, E.M. (2002). Quantitative assays for GTPase-activating proteins. *Methods Enzymol* 344, 601-617.
72. Chenna, R., Sugawara, H., Koike, T., Lopez, R., Gibson, T.J., Higgins, D.G., and Thompson, J.D. (2003). Multiple sequence alignment with the Clustal series of programs. *Nucleic Acids Res* 31, 3497-3500.

## Figures and Tables

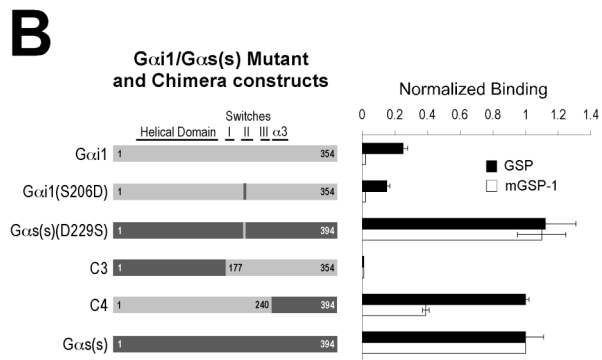
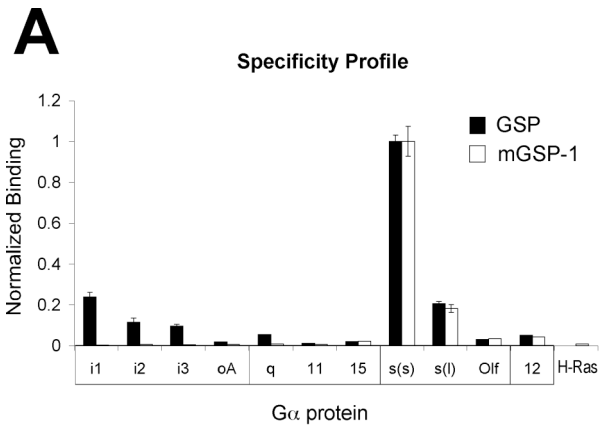
**Figure 5.1 Directed evolution selection scheme.** (A) mRNA-display selection cycle. A dsDNA library (pool 0) is synthesized containing an invariant T7 promoter, untranslated region (UTR) and open reading frame (ORF). Template DNA is transcribed (1), ligated to puromycin via a 3'-DNA-tether (2) and translated (3) to generate mRNA-peptide fusions, individually composed of a peptide linked to its corresponding mRNA genotype (black) via puromycin (P). Purified fusions are reverse transcribed (4) prior to selection on a solid phase target (Gas(s)-beads). PCR amplification of cDNA retained on the target (5) produces dsDNA template (pool 1) for the subsequent round of selection. (B) Scheme for positive selection (R6A-1-library:Gas(s)-beads): The R6A-1-library sequence is listed; residues in bold are doped with a 50% mutation rate and random residues are represented as Xs. At left is a plot of pool enrichment for the positive selection: RNase treated [<sup>35</sup>S]Met-peptide fusions from iterative rounds of selection are assayed for pull-down on Gas(s)-beads (black vertical bars) with background binding to neutravidin-beads < 0.5%. At right, individual peptide sequences from pool 8 are screened for their ability to bind soluble Gαi1 (gray horizontal bars) and Gas(s) (black horizontal bars). Conserved residues in selected peptides are boxed in gray. (C) Scheme for maturation selection (GSP-library:Gas(s)-beads with Gαi1 competitor): At left, enrichment of pool binding to Gas(s)-beads (black vertical bars) is contrasted with binding to Gαi1-beads (gray vertical bars). Selected peptides from pool 6 bind specifically to Gas(s) in the Gα-binding screen.



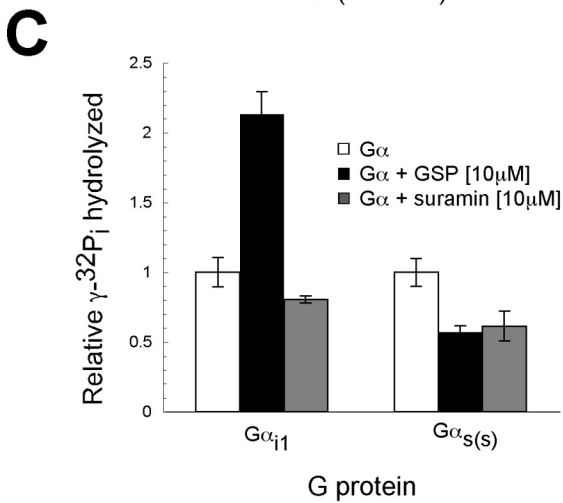
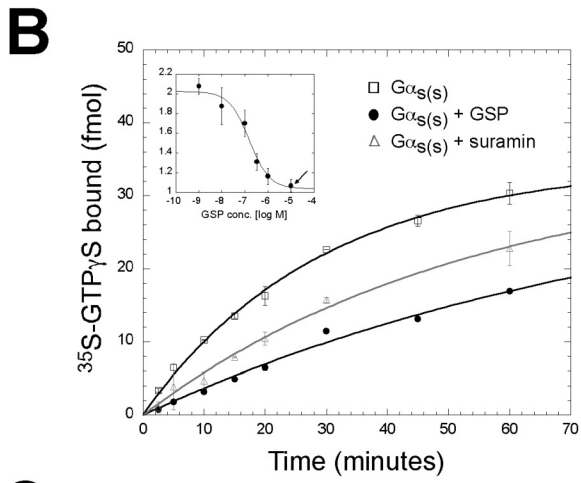
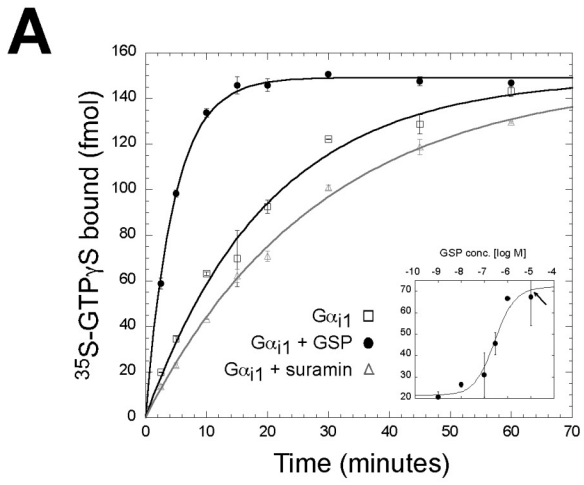
**Figure 5.2 SPR binding data for the GSP-G $\alpha$ s(s) complex.** A concentration series of GSP peptide is injected (200  $\mu$ L at 0s, with a 100  $\mu$ L/min flow rate) across  $\sim$ 1000 RU of G $\alpha$ s(s) immobilized on a streptavidin biosensor chip. Global kinetic fits (black) are overlaid on the sensogram data (gray). Two sensogram plots at 90 nM GSP and three plots at 0 nM demonstrate data precision. The derived binding constant is shown in Table 5.1.



**Figure 5.3 G $\alpha$ -binding specificity profiles and mutational analysis.** (A) GSP and mGSP-1 peptides are assayed for binding to a profile of 11 G $\alpha$  proteins and the small GTPase H-Ras, boxed by class along the x-axis of the plot. Binding is a measure of [<sup>35</sup>S]Met-G $\alpha$  protein pull-down on peptide-beads performed at 4 °C. Control pull-down on MBP-neut beads shows no binding (< 0.01) and presence of aluminum fluoride abrogates pull-down for both peptides. Error bars represent S.D. for multiple experiments. (B) Mutational analysis: Previously characterized G $\alpha$ i1/G $\alpha$ s(s) reciprocal mutants and chimeras were assayed for pull-down on GSP and mGSP-1 peptide-beads. GSP and mGSP-1 exhibit increased binding to the C4 G $\alpha$  chimera containing the  $\alpha$ 3 and  $\alpha$ 3- $\beta$ 5 effector loop of G $\alpha$ s(s). Chimera constructs are depicted at left [36]: G $\alpha$ i1 sequence is shown in light gray and G $\alpha$ s(s) sequence, numbered in the G $\alpha$ s(l) convention, is shown in dark gray.



**Figure 5.4 GSP nucleotide exchange assays.** **(A)** Time course of [<sup>35</sup>S]GTPγS binding to 50 nM Gαi1 at 30 °C in the presence of 10 μM GSP or 10 μM suramin. Data are fit to a single exponential association curve to give apparent rates of GTPγS association: Gαi1  $0.050 \pm 0.005 \text{ min}^{-1}$ ; + GSP  $0.214 \pm 0.007 \text{ min}^{-1}$ ; + suramin  $0.034 \pm 0.002 \text{ min}^{-1}$ . Plots are normalized for maximum binding values with error bars representing S.D. of two measurements acquired during the same experiment. A dose response curve is shown in the inset plot for 50 nM Gαi1 incubated with the indicated concentration of GSP for 2.5 min. A logistic fit of the data gives an EC50 value of  $290 \pm 8 \text{ nM}$ . Arrows indicate the concentration of peptide used in the time course measurements. **(B)** Time course of [<sup>35</sup>S]GTPγS binding to 50 nM Gαs(s) at 20 °C in the presence of 10 μM GSP or 10 μM suramin. GTPγS association rates: Gαs(s)  $0.034 \pm 0.003 \text{ min}^{-1}$ ; + GSP  $0.011 \pm 0.004 \text{ min}^{-1}$ ; + suramin  $0.018 \pm 0.003 \text{ min}^{-1}$ . The inset GSP-Gαs(s) dose response curve gives an IC50 value of  $157 \pm 4 \text{ nM}$ . **(C)** Steady-state hydrolysis is measured by inorganic phosphate [<sup>32</sup>P<sub>i</sub>] released from the reaction of 100 nM Gα, with [<sup>32</sup>P]GTP in the presence of 10 μM GSP or 10 μM suramin. Error bars indicate S.D. of multiple measurements.

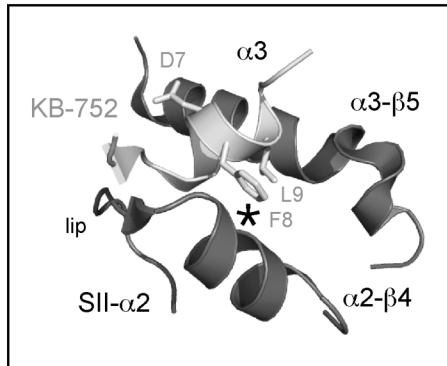
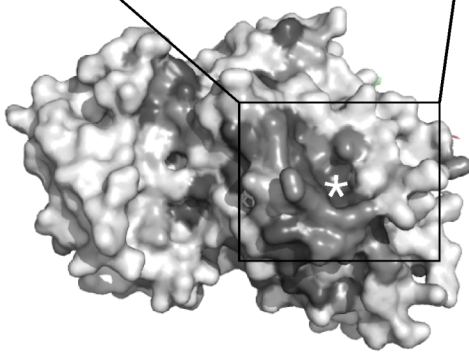


**Figure 5.5 Structural analysis of peptide-G $\alpha$  recognition.** (A) Sequence alignment of R6A-1, GSP, mGSP-1, mGSP-2, and KB-752: identical GSP core residues are highlighted in gray boxes and conserved residues in light gray; residues in the KB-752-G $\alpha$ i1 crystal structure are underlined. (B) Ribbon diagram of KB-752 (light gray) binding within the SII/ $\alpha$ 3 cleft of G $\alpha$ i1 (slate). The asterisk denotes an invariant hydrophobic binding pocket composed of G $\alpha$ i1 residues R208, W211, I212, F215, L49, and I253 [32]. Structural image was made from Protein Data Bank file 1Y3A [13]. KB-752 consensus motif residues DFL are labeled (light gray) along with structural elements of G $\alpha$ i1 (slate). (C) Molecular surface representation of G $\alpha$  protein sequence homology superimposed on the G $\alpha$ s(s)-GTP $\gamma$ S crystal structure. A sequence alignment of G $\alpha$  proteins (i1, i2, i3, oA, q, 11, 15, s(s), Olf, and 12) was performed by ClustalW [72] generating a list of variable (near white), similar (light gray), conserved (gray), and identical (dark gray) G $\alpha$  residues, which were grafted onto the G $\alpha$ s(s)-GTP $\gamma$ S crystal structure. The asterisk denotes an invariant hydrophobic binding pocket within the SII/ $\alpha$ 3 cleft. (D) Three G $\alpha$  binding models- Superimposition of (1) RGS (RGS4 [29]: dotted black line), (2) GoLoco (GoLoco/GPR [31]: black line), and (3) effector (AC VC<sub>1</sub>/IIC<sub>2</sub> [41]: white line) binding footprints on G $\alpha$ . The footprints overlap at the conserved SII and SII/ $\alpha$ 3 cleft of G $\alpha$ . G $\alpha$ s(s) residue Asp229 implicated in RGS binding specificity is highlighted in gray. Binding surfaces were grafted onto the structure of G $\alpha$ s(s) to generate the image. Structural images for (C) and (D) were made from the Protein Data Bank file 1AZT [41] using PyMOL (<http://www.pymol.org>).

**A**

R6A-1		DQLYWWEYL	
GSP	MAMSDRN	KRLTVWEFL	ALPSST
mGSP-1	MAMSDQN	KRMTVREFL	ALPSSL
mGSP-2	MYTSDHN	KLLTVREFL	ALPSST
KB-752		SRVTWYDFL	MFDTKSR

-5      0      1                      9                      15

**B****C**

variable  conserved

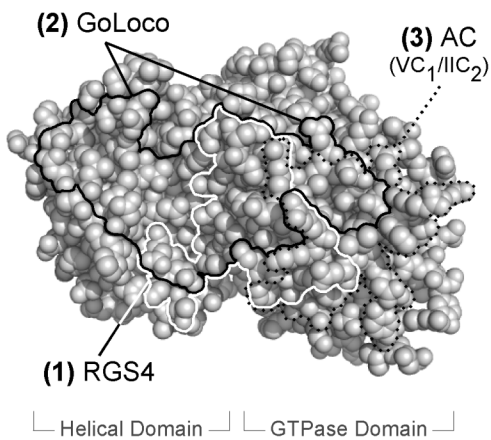
**D**

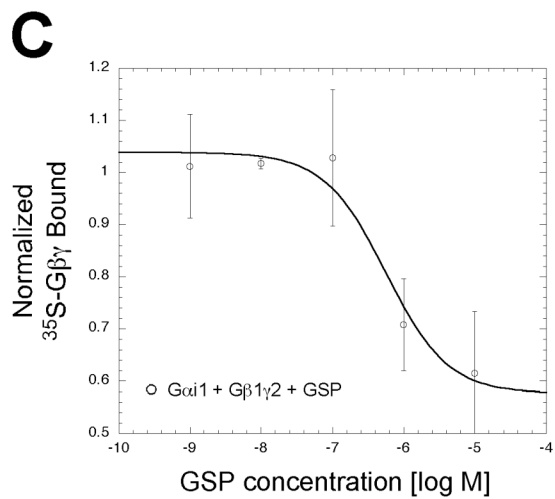
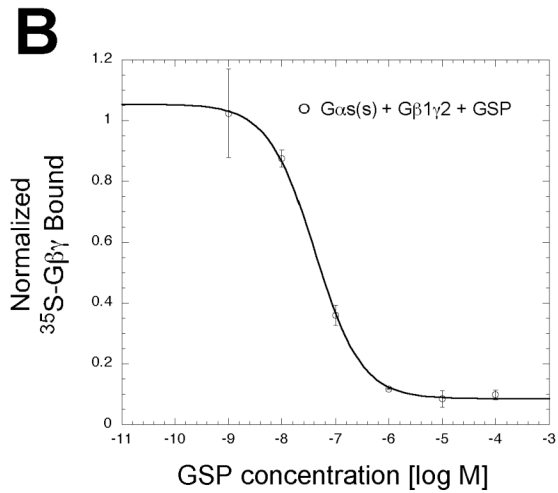
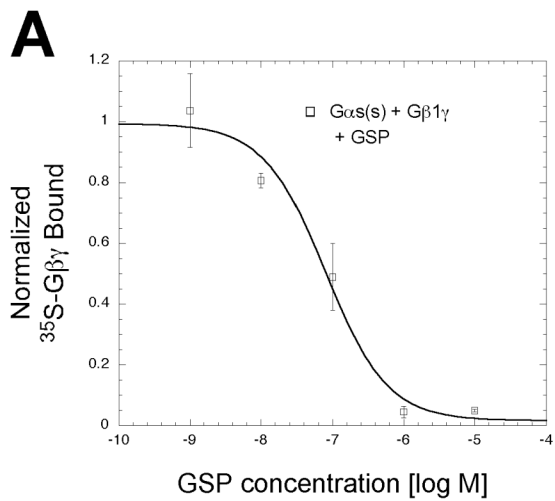
Table 5.1: Peptide-G $\alpha$ dissociation constants ( $K_D$ ) and G $\alpha$ (s) binding specificity ( $G\alpha(s)$ - $\Delta\Delta G$ ) values.				
peptide	$K_D$ (nM)		$G\alpha(s)$ - $\Delta\Delta G$ (kcal mol <sup>-1</sup> )	
	G $\alpha$ i1	G $\alpha$ (s)		
R6A <sup>a</sup>	60		NA	
R6A-1 <sup>b</sup>	200	50,000	-3.3	
GSP	280 $\pm$ 40	100 $\pm$ 15	0.5	
mGSP-1	10,300	300	2.1	
mGSP-2	4,400 $\pm$ 220	130	2.1	

$K_D$  values, calculated from kinetic parameters ( $k_d/k_a$ ), are given  $\pm$  S.D. when more than one independent measurement has been made.  
 $G\alpha(s)$ - $\Delta\Delta G$  values are calculated as  $G\alpha(s)$ - $\Delta\Delta G = [\Delta G^\circ(\text{peptide-G}\alpha\text{i1}) - \Delta G^\circ(\text{peptide-G}\alpha(s))]$ , where  $\Delta G^\circ = -RT \ln K_{obs}$ .  
<sup>a</sup>R6A and <sup>b</sup>R6A-1 binding constants are previously published values [12, 27]. The R6A peptide sequence is MSQTKRLD DQLYWWEYL.



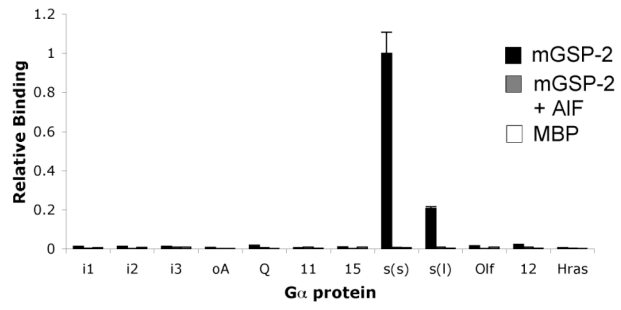
## ***Supplemental Figures***

**Figure S5.1 Heterodimer pull-down assays.** GSP disrupts heterotrimer formation in  $G\alpha s(s)$  and  $G\alpha i1$ . **(A)** Equilibrium pull-down of  $G\beta 1\gamma 1$  on  $G\alpha s(s)$ -beads over a GSP concentration series.  $G\beta 1\gamma 1$  is co-translated, confirmed by SDS-gly-PAGE, and incubated with a solution of  $G\alpha s(s)$ -neut + peptide. Curves are fit to a 3-parameter logistic equation to calculate an  $IC_{50}$  value for  $G\alpha\beta\gamma$  disruption.  $IC_{50}$  values are fit for **(A)**  $G\alpha s(s)$ - $G\beta 1\gamma 1$  + GSP ( $80 \pm 2$  nM); **(B)**  $G\alpha s(s)$ - $G\beta 1\gamma 2$  + GSP ( $41 \pm 2$  nM); and **(C)**  $G\alpha i1$ - $G\beta 1\gamma 2$  ( $564 \pm 21$  nM).

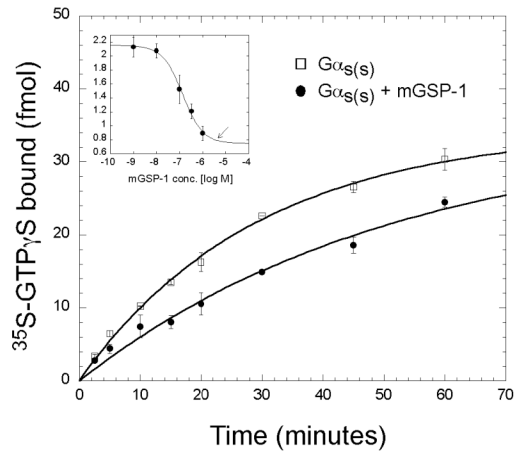
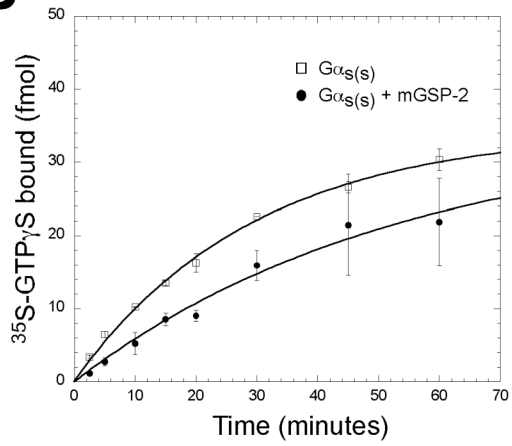


**Figure S5.2 G $\alpha$ -specificity profile for mGSP-2.** G $\alpha$  Specificity Profile. The mGSP-2 peptide is assayed for binding to a profile of 11 G $\alpha$  proteins, representing the 4 different classes of G $\alpha$ , and the small GTPase H-Ras. Binding is a measure of [<sup>35</sup>S]Met-G $\alpha$  protein pull-down on peptide-beads performed at 4 °C. Two controls are shown: pull-down in the presence of aluminum fluoride (gray bars) and pull-down on MBP-neut-beads (white bars); both controls show nominal binding (< 0.01). Error bars represent S.D. for multiple experiments.

**A**



**Figure S5.3 mGSP nucleotide exchange assays.** mGSP-1 and mGSP-2 inhibit nucleotide exchange in  $G\alpha s(s)$ . **(A)** [ $^{35}\text{S}$ ]GTP $\gamma$ S binding to 50 nM  $G\alpha s(s)$  at 20 °C in the presence of 5  $\mu\text{M}$  mGSP-1. Data are fit to a single exponential association curve to give apparent rates of GTP $\gamma$ S association:  $G\alpha s(s)$   $0.041 \pm 0.004 \text{ min}^{-1}$ ; + mGSP-1  $0.019 \pm 0.005 \text{ min}^{-1}$ . Plots are normalized for maximum binding values with error bars representing S.D. of two measurements acquired during the same experiment. A dose response curve is shown in the inset plot for 50 nM  $G\alpha s(s)$  incubated with the indicated concentration of mGSP-1 for 2.5 min. A logistic fit of the data gives an IC<sub>50</sub> value of  $102 \pm 3 \text{ nM}$ . **(B)** Time course of [ $^{35}\text{S}$ ]GTP $\gamma$ S binding to 50 nM  $G\alpha s(s)$  at 20 °C in the presence of 5  $\mu\text{M}$  mGSP-2. GTP $\gamma$ S association rates:  $G\alpha s(s)$   $0.041 \pm 0.004 \text{ min}^{-1}$ ; + mGSP-2  $0.020 \pm 0.005 \text{ min}^{-1}$ . **(C)** Steady-state hydrolysis is measured by inorganic phosphate [ $\gamma^{32}\text{P}_i$ ] released from the reaction of 100 nM  $G\alpha$ , with [ $\gamma^{32}\text{P}$ ]GTP in the presence of 5  $\mu\text{M}$  mGSP-1 or 5  $\mu\text{M}$  mGSP-2. Error bars indicate S.D. of multiple measurements.

**A****B****C**